PHYSICAL REVIEW E, VOLUME 65, 030701

Dramatic effect of an additional CH_2 group on the temperature variation of the Sm-C^*_α short helical pitch

A. Cady,[1] D. A. Olson,[1] X. F. Han,[1] H. T. Nguyen,[2] and C. C. Huang[1]
[1]*School of Physics and Astronomy, University of Minnesota, Minneapolis, Minnesota 55455*
[2]*Centre de Recherche Paul Pascal, CNRS, Université Bordeaux I, Avenue A. Schweitzer, F-33600 Pessac, France*
(Received 7 November 2001; published 27 February 2002)

High-resolution differential optical reflectivity was used to study the temperature evolution of the short helical pitch in the Sm-C^*_α phase of successive members from two liquid-crystal homologous series. With the addition of one CH_2 group, the magnitude and temperature evolution of the pitch change dramatically, and the molecular arrangements between consecutive surface layers found in free-standing films change from being anticlinic to synclinic.

DOI: 10.1103/PhysRevE.65.030701 PACS number(s): 61.30.Gd, 77.84.Nh, 83.80.Xz

Soon after the discovery of the antiferroelectric phase (Sm-C^*_A) in one liquid-crystal compound, the existence of a new mesophase (Sm-C^*_α) intermediate between the Sm-*A* and the Sm-*C** was reported by Fukui *et al.* [1]. Similar to the Sm-C^*_A and Sm-*C** phases, the liquid-crystal molecules in the Sm-C^*_α phase form a layered structure in which the molecules have a finite tilt relative to the layer normal but no long range positional order. Considerable experimental effort has been aimed at characterizing the molecular azimuthal arrangements in the Sm-C^*_α phase as well as at determining the interactions between layers that cause the complicated chiral smectic-phase sequences. Applying an electric field to their sample, Hiraoka *et al.* [2] observed stepwise increases in apparent tilt angle in the Sm-C^*_α phase of one liquid-crystal compound. The devil's staircase model [3] was proposed to account for the observed successive structure changes with arbitrarily large modulation lengths. Instead by employing resonant x-ray scattering, Mach *et al.* [4] showed that the Sm-C^*_α phase exhibits an incommensurate short-helical-pitch (ISHP) structure. The existence of ISHP has been confirmed by optical studies from two research groups [5,6]; however, the results from different compounds differed in the magnitude and temperature evolution of the ISHP. The overwhelming experimental evidence supports the ISHP structure.

Although chirality is an important symmetry-breaking factor in getting the complicated phase sequences exhibited by some liquid crystals, it is too weak an effect to cause ISHP. A more plausible explanation for the existence of ISHP is frustration resulting from the competition between nearest-neighbor and next-nearest-neighbor interlayer interactions. Such interactions can be either ferroelectric or antiferroelectric, and both interactions have in fact been observed in the surface structures of free-standing films exhibiting the Sm-C^*_α phase [5–7]. In this paper, two very different temperature variations of ISHP in the Sm-C^*_α phase from successive members of two liquid-crystal homologous series are reported. Employing a simple free-energy expansion up to the next-nearest-neighbor interaction term, we demonstrate that competition between nearest-neighbor ferroelectric interactions and next-nearest-neighbor antiferroelectric interactions explains the temperature evolution of ISHP very well.

We will present data from detailed optical investigations of two liquid-crystal compounds from one homologous series. The general molecular structure of these compounds, 10- and 11-OHFBBB1M7, is shown in Fig. 1. For the rest of this paper, we will use the abbreviated names: 10OHF and 11OHF. Upon cooling, the phase sequences are isotropic (*I*) (124°C), Sm-*A* (86°C), Sm-C^*_α (75°C), Sm-*C** (67°C) crystal (Cr) for 10OHF and *I* (120°C), Sm-*A* (95.8°C), Sm-C^*_α (93.2°C), Sm-*C** (75°C) Cr for 11OHF as reported in [8] and from our optical studies [9]. The addition of one CH_2 group in the alkyl-chain without the chiral group produces a large decrease in the Sm-C^*_α phase range from 11 K in 10OHF to 2.6 K in 11OHF. Our high-resolution differential optical reflectivity (DOR) measurements reveal a dramatic difference in the temperature variation of ISHP between these two compounds. A similar difference also occurs in the $n=10$ and $n=11$ members of the *n*OTBBB1M7 homologous series (10OT and 11OT), whose molecular structure is shown in [4].

Since the Sm-C^*_α phase is optically uniaxial, we need a probe that is sensitive to surface orientations. In addition, the Sm-C^*_α structure changes rapidly with temperature and thus necessitates a fast experimental probe. Our DOR measurements on free-standing films, which can be taken roughly ten times as fast as ellipsometry measurements, satisfy both of these constraints, making it an excellent probe for studying the Sm-C^*_α phase.

The films were prepared in a two-stage oven with a temperature resolution of 10-mK and a 0.7-atm helium exchange gas. The films were drawn across a 7-mm diameter circular hole in a glass coverslip with two electrodes on opposite sides of the opening allowing the application of an electric field in the plane of the film. The data was acquired during temperature ramps of 50–80 mK/min under an applied electric field of ≈ 3 V/cm.

Details of our DOR setup can be found in [10]. We deter-

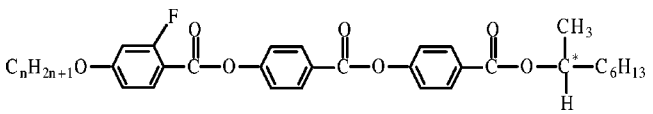

FIG. 1. The molecular diagram of *n*OHFBBB1M7.

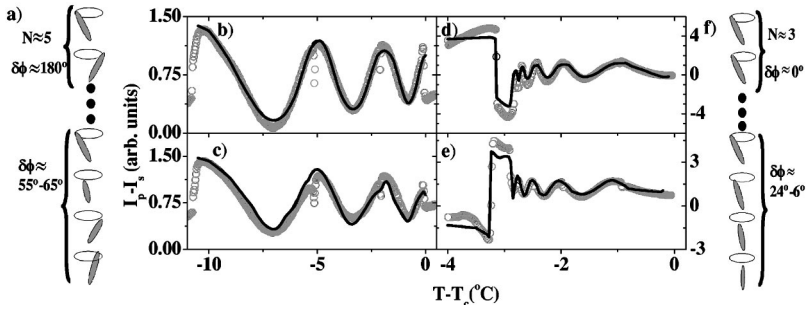

FIG. 2. (a) and (f) show cartoons of the ISHP with surface layers found in 10OHF and 11OHF, respectively. N is the number of surface layers on each surface and $\delta\phi$ is the interlayer azimuthal angle. (b) and (c) show data (circles) obtained from a 116-layer 10OHF film during temperature ramps of 80 mK/min, through the Sm-C_α^* phase with opposite applied electric fields of 3 V/cm applied in the plane of the film and in the incidence plane. (d) and (e) show data (circles) acquired from a 115-layer 11OHF film in its Sm-C_α^* phase range under the same conditions as for (b) and (c). In all four cases, the simulations are shown as solid lines.

mine the film thickness by employing two lasers with wavelengths of 6328 Å and 5435 Å and measuring the reflectivity of the film as a function of incident angle in the Sm-A phase. We simulate the data using the Sm-A layer spacing d and the ordinary index of refraction n_o, as measured by our null-transmission ellipsometry (NTE). The accuracy of the measurement is ± 1 layer for films up to 100 layers and ± 2 layers for thicker films.

The DOR signal is obtained using chopped intensity-stabilized 6328-Å He:Ne laser light. The incident beam is polarized by a Glan-Thompson polarizer mounted on a rotating stage. The light reflected by the film is split into two beams, each having only the p- or s-polarization state, by a polarizing beam splitter before being directed into separate photodetectors where the respective intensities, I_p and I_s, are measured. The currents resulting in the two detectors are immediately subtracted, converted to voltage, amplified, and sent to a lock-in amplifier, yielding the $I_p - I_s$ signal. In addition the current to voltage converter outputs I_p and $-I_s$ separately to another lock-in that gives the total reflected intensity $I_p + I_s$. The experiment is begun by raising the temperature of the film into the uniaxial Sm-A phase and rotating the Glan-Thompson polarizer until the $I_p - I_s$ signal is zero. Then upon cooling the film into the Sm-C_α^* phase we measure the temperature variation of $I_p - I_s$ and $I_p + I_s$.

In the Sm-C_α^* phase, as the ISHP evolves with temperature the surface layers linked to the interior helix rotate. The surface layers provide the optical biaxiality needed to probe the layer structure. As the surface layers rotate about the layer normal the $I_p - I_s$ signal oscillates, corresponding to the changing polarization of the reflected laser light. During each rotation of the structure the net polarization of the film goes to zero, resulting in a spike in the $I_p - I_s$ signal as the film reorients rapidly by 180°.

Our DOR data from a 116-layer 10OHF film and a 115-layer 11OHF film are shown in Fig. 2 for both orientations of the applied electric field. Both data (circles) sets display the above-mentioned features. We studied 18 10OHF films ranging from 24 to 508 layers, 7 films of 11OHF ranging from 42 to 128 layers, and several films of 10OT and 11OT. For all the compounds, the number of oscillations increases linearly with film thickness indicating that these oscillations are related to structural changes in the film's interior layers. To conserve space, we only present data from the nOHF compounds.

Although the $I_p - I_s$ signal shows some similar features for both compounds, the frequency f of the oscillations in temperature space are very different. For 10OHF and 10OT, f shows a slight decrease on cooling whereas f increases considerably on cooling for 11OHF and 11OT. The f is related to how fast the ISHP changes with temperature. For a given film thickness, a fast increase in the ISHP will cause the surface layers to rotate quickly thus giving more oscillations in the $I_p - I_s$ signal than if the pitch is increasing more slowly. As clearly shown by the 10OHF data in Figs. 2(b) and 2(c), the rate of change of the pitch on cooling is rather steady because f does not change significantly. In the 11OHF data shown in Figs. 2(d) and 2(e), however, f increases signifiantly on cooling, indicating a more rapid change in the pitch.

As shown in Figs. 2(b) and 2(c), the DOR signals acquired from the 10OHF films are almost unchanged, in both magnitude and location of the oscillations, by switching the direction of the applied electric field. This feature is similar to that found in studies of the 10OT compound [5] and indicate an anticlinic surface-layer arrangement. The data aquired from the 11OHF films are shown in Figs. 2(d) and 2(e). The amplitude of the signal and the locations of the oscillations are different for opposite orientations of the electric field, implying a synclinic surface-layer arrangement. These features do not depend on the film thickness but result from the surface layers in the free-standing films as discussed below.

The 4×4 matrix method was used to simulate our data. Simulations are shown as solid lines in Fig. 2. Three essential parameters d, n_0, and the extraordinary index of refraction n_e are obtained from our NTE. For 10OHF $d = 39.4 \pm 0.1$ Å, $n_0 = 1.469 \pm 0.005$, and $n_e = 1.595 \pm 0.01$. Moreover by plotting the film thickness in layers versus the number of oscillations in the $I_p - I_s$ signal, and fitting to a line, we obtain a y-intercept of 10.2 ± 2 layers. All the 10OHF data are fitted well using five anticlinic layers on each surface. For 11OHF, $d = 39.6 \pm 0.1$ Å, $n_0 = 1.467 \pm 0.005$,

and $n_e = 1.595 \pm 0.01$. Similarly, three synclinic layers on each surface was found for 11OHF.

By measuring the value of the helical pitch at one end of the Sm-C^*_α phase and performing simulations of the data, we can use the oscillations described above to find the ISHP throughout the Sm-C^*_α phase. Two methods were used to determine the starting (ending) pitch of 10OHF (11OHF) on cooling. For 10OHF, the periodicity of the $I_p - I_s$ signal was found to be 6.5 ± 0.5 smectic layers near the Sm-A–Sm-C^*_α transition after studying many films with consecutive thicknesses ranging from 44 to 56 layers [11]. For 11OHF the pitch is too large to make the previous method practical. However, the optical properties appear to evolve continuously from the Sm-C^* phase. This is further supported by recent resonant x-ray measurements of the ISHP from another compound [12]. Thus, the pitch was determined to be 65 ± 5 layers below the Sm-C^*–Sm-C^*_α transition using NTE. Both ellipsometric parameters Ψ and Δ are obtained as a function of applied electric field orientation angle α. The fitting to both $\Psi(\alpha)$ and $\Delta(\alpha)$ allow us to determine the size of the optical pitch in the Sm-C^* phase.

The pitches at other temperatures were found by simulating the data until both the maxima and the minima of the simulated $I_p - I_s$ values matched the measured values. The positions of these maxima and minima were strongly dependent on the rate of change of the pitch values used. The amplitude of the oscillations is determined by the biaxiality of the structure that arises from the tilted surface layers, the tilt of the interior layers, and the film reflectivity. The relatively small continuous change in amplitude of the oscillations in the $I_p - I_s$ signal demonstrates that the number of surface layers is constant, but the surface tilt increases on cooling as expected. Thus fits were done without varying the number of surface layers. The tilt and the reflectivity can be found by fitting the total reflected intensity of the film $I_p + I_s$, at the 17.5° angle of incidence. The average value of the $I_p - I_s$ signal is affected by angle between the polarization of the incident light and the applied electric field direction, which was recorded during the experiment.

For clarity, the temperature variations of ISHP from two representative films of each compound are shown in Fig. 3. ISHP results are reproduced with other film thicknesses. The relative resolution of the pitch shown in Fig. 3 was less than 0.1 layers. The results show a clear difference in the evolution of the ISHP in these two compounds. Upon cooling toward the Sm-C^*_α–Sm-C^* transition, the pitch decreases gradually to 5.5 layers for 10OHF. In constrast, for 11OHF, the pitch increases gradually at first, then rapidly, and appears to change continuously to ≈ 65 layers in the Sm-C^* phase. Cartoons of the ISHP structures with surface layers are shown in Figs. 2(a) and 2(f) for 10OHF and 11OHF, respectively.

To analyze the pitch evolution found from the data, we employed the following free-energy expansion due to interlayer interactions up to the next-nearest-neighbor term

$$G = \frac{1}{2} \sum_{j=1}^{N} [a_1(\vec{\xi}_j \cdot \vec{\xi}_{j+1}) + a_2(\vec{\xi}_j \cdot \vec{\xi}_{j+2})]. \qquad (1)$$

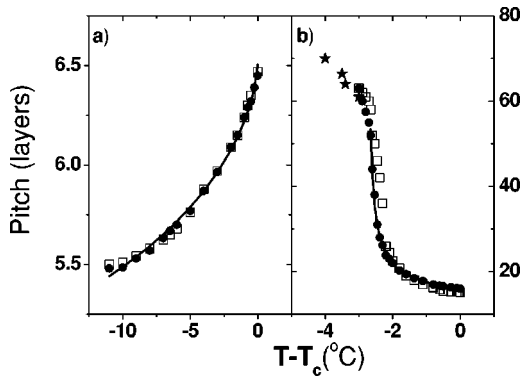

FIG. 3. (a) and (b) show the different pitch evolutions used in simulating the 10OHF and the 11OHF ($I_p - I_s$) data, respectively. In (a) circles are from a 508-layer film and the squares are from a 116-layer film. In (b) circles are from a 121-layer film and squares are from a 115-layer film. The stars represent ellipsometry measurements. Solid lines are fits to the model.

Here, $\vec{\xi}_j$ $[= \theta_j(\cos\phi_j, \sin\phi_j)]$ is the two-dimensional order parameter describing the magnitude θ_j and direction ϕ_j of the molecular tilt in the jth layer and N is the number of smectic layers. The coefficients a_1 and a_2 represent the strength of the nearest-neighbor and next-nearest-neighbor interactions, respectively. Because of the large tilt angle θ variation throughout the Sm-C^*_α phase, we used the extended mean field result for which θ is assumed to have the form $\theta = A[(T_c - T)/T_c]^{0.33}$ [13]. We also expand a_1 and a_2 to second order in θ as $a_1 = -a + b\theta^2$ and $a_2 = c + d\theta^2$ where a, b, c, and d are temperature-independant quantities. The chiral interaction terms and interactions up to fourth nearest neighbors have been included in other expansions to explain the existence of the other Sm-C^* variant phases [14]. From fitting our pitch data, we have found that the competition between nearest-neighbor and next-nearest-neighbor interactions is reponsible for the ISHP structure. Beyond selecting the handedness of the ISHP, no chiral terms are necessary.

By minimizing G, we find the approximate solution for the change in the azimuthal angle to be $\delta\phi = \arccos[(a - b\theta^2)/4(c + d\theta^2)]$. The pitch in smectic layers is $2\pi/\delta\phi$. The fits to the pitches as functions of temperature are shown in Fig. 3 as solid lines. For 10OHF, the fitting yields $bA^2/a = 2.0 \pm 0.3$, $dA^2/a = 0.5 \pm 0.15$, and $c/a = 0.44 \pm 0.02$. For 11OHF, the results are $bA^2/a = 20.71 \pm 0.10$, $dA^2/a = -5.73 \pm 0.03$, and $c/a = 0.271 \pm 0.001$. For both compounds $a_1 < 0$, indicating ferroelectric coupling of nearest neighbors, and $a_2 > 0$, representing antiferroelectric coupling of next-nearest neighbors. Both a_1 and a_2 increased slightly toward the Sm-C^* transition in the 10OHF compound. The small change in the interactions corresponds to the small change in the pitch. In 11OHF, both a_1 and a_2 changed more significantly, both approaching zero on cooling to the Sm-C^* phase. The transition temperature for the Sm-C^*–Sm-C^*_α given as 93.2°C in the phase sequence corresponds to the inflection point of the pitch in Fig. 3(b).

The ISHP of the Sm-C^*_α phase has been studied in great detail as a function of temperature for two liquid-crystal compounds. We have shown that the addition of a single

CH_2 group to the alkyl chain without the chiral group of a liquid-crystal compound can greatly affect the temperature evolution of the pitch.

The pitch in 11OHF appears to evolve continuously on cooling to the Sm-C^* phase. The absence of any detectable jump in the pitch in our data and in recent resonant x-ray results from another compound [12] suggest the possibility of a continuous evolution of the pitch from the Sm-C^*_α to the Sm-C^* phase. Since both phases have the same symmetry, the transition should be similar to the well-known liquid-gas transition. Generally such a transition without symmetry breaking will cross a first-order transition line or exhibit a continuous evolution of some physical parameters, e.g., the helical pitch in the Sm-C^*–Sm-C^*_α transition. Between these two cases, the first-order transition line will end at a critical point. It is important to characterize physical properties near this critical point.

We have found that a free-energy expansion including up to next-nearest-neighbor interlayer interactions fits our results extremely well. The results suggest that the Sm-C^*_α phase arises from frustration resulting from the competition between nearest-neighbor and next-nearest-neighbor interlayer interactions. Another important observation is that there are two types of the Sm-C^* phase. The conventional one has a micron-size pitch that is mainly caused by chirality of the molecules. The other one has a much shorter pitch, similar to the one found in 11OHF, which requires the consideration of interplay of the chirality, nearest-neighbor and next-nearest-neighbor interlayer interactions and possibly other terms.

We would like to thank Dr. R. Pindak for numerous discussions. This research was supported in part by the National Science Foundation, Solid State Chemistry Program under Grant Nos. DMR-9703898, 9901739, and INT-9815859.

[1] M. Fukui, H. Orihara, Y. Yamada, N. Yamamoto, and Y. Ishibashi, Jpn. J. Appl. Phys., Part 2 **28**, L849 (1989).
[2] K. Hiraoka, Y. Takanishi, K. Skarp, H. Takezoe, and A. Fukuda, Jpn. J. Appl. Phys., Part 2 **30**, L1819 (1991).
[3] A. Fukuda, Y. Takanishi, T. Isozaki, K. Ishikawa, and H. Takezoe, J. Mater. Chem. **4**, 997 (1994).
[4] P. Mach, R. Pindak, A.-M. Levelut, P. Barois, H.T. Nguyen, C.C. Huang, and L. Furenlid, Phys. Rev. Lett. **81**, 1015 (1998).
[5] P.M. Johnson, S. Pankratz, P. Mach, H.T. Nguyen, and C.C. Huang, Phys. Rev. Lett. **83**, 4073 (1999).
[6] D. Schlauf, Ch. Bahr, and H.T. Nguyen, Phys. Rev. E **60**, 6816 (1999).
[7] D.A. Olson, S. Pankratz, P.M. Johnson, A. Cady, H.T. Nguyen, and C.C. Huang, Phys. Rev. E **63**, 061711 (2001).
[8] V. Faye, J.C. Rouillon, C. Destrade, and H.T. Nguyen, Liq. Cryst. **19**, 47 (1995).
[9] Our optical studies on free-standing films indicate that the phase below the SmC^*_α may be a ferrielectric phase in 10OHF.
[10] S. Pankratz, P.M. Johnson, and C.C. Huang, Rev. Sci. Instrum. **71**, 3184 (2000).
[11] Although the accuracy of the thickness measurement is ± 1 layer, we can easily differentiate incremental differences of one layer.
[12] Preliminary results from a recent resonant x-ray run.
[13] C.C. Huang and J.M. Viner, Phys. Rev. A **25**, 3385 (1982).
[14] M. Čepič and B. Žekš, Phys. Rev. Lett. **87**, 085501 (2001).